20

Photoinduced change of $AgInS_2$ quantum dots fluorescence properties: influence of protein environment

© V.I. Gorbacheva[1], I.A. Reznik[2], E.P. Kolesova[1]

[1] Sirius University of Science and Technology, Sirius Federal territory, Krasnodar Krai, Russia
[2] ITMO University, 197101 St. Petersburg, Russia

e-mail: e.p.kolesova@gmail.com

Received November 11, 2024
Revised April 28, 2025
Accepted April 28, 2025

Semiconductor quantum dots (QDs) $AgInS_2$ and $AgInS_2$/ZnS were synthesized and changes in their fluorescence properties under external radiation were studied. To assess the effect of the protein environment, QDs were encapsulated in albumin nanoparticles and coated with a fetal bovine serum shell to imitate the protein corona. It was demonstrated that the protein environment has a significant effect on the luminescent properties of QDs, namely, a hypsochromic shift of the luminescence band and a decrease in the luminescence quantum yield. The results showed that ZnS shell and both types of protein shells lead to a decrease in the photobleaching rate of the fluorescent properties of QDs as a result of interaction with light.

Keywords: quantum dots, fluorescence, photoinduced processes, protein corona, albumin nanocarriers.

DOI: 10.61011/EOS.2025.04.61418.7311-24

Introduction

In the years passed since their colloidal synthesis, semiconductor quantum dots (QDs) have attracted research attention due to their unique photophysical properties and the size quantization effect [1]. Traditional A2B6 QDs have found application both in biomedicine for biological imaging and sensorics and as efficient donors of energy and charge carriers in complexes with various molecules [2]. However, these QDs are highly toxic [3]. Biologists are concerned about the presence of heavy metal ions (namely Cd, Se, Zn, and Pb), which may cause oxidative stress and DNA destruction, in QDs [4]. Owing to their relatively simple synthesis and high stability and luminescence quantum yield, $AgInS_2$ ternary QDs have become a promising alternative to traditional QDs in medical applications [5]. In addition, QDs of this kind have the capacity to generate a superoxide independently and act as a sensitizer for photodynamic therapy [6]. Thus, $AgInS_2$ QD-based platforms may be used both for cell imaging and biodistribution of systems in the body and as a therapeutic tool. In both these cases, the functionality of QDs depends on the results of QD–radiation interaction.

QDs belong to the class of photoactivated systems the photophysical properties of which may change after interaction with light. When external radiation is absorbed, photochemical reactions proceed on the particle surface (specifically, surface photooxidation) [7]. In the case of traditional CdSe QDs, the fluorescence quantum yield increases at the first stage due to the oxidation of defects on the QD surface that compete with fluorescence. Further surface oxidation leads to the formation of new defects, which results in deterioration of the fluorescent properties of QDs.

We have demonstrated in our earlier study that photoinduced processes may enhance both the fluorescent properties of QDs and their efficiency as a charge donor in a system with titanium dioxide nanoparticles (NPs) [8]. It is fair to assume that photoinduced processes should also have a significant impact on the properties of $AgInS_2$ QDs, but this issue has not been investigated in sufficient detail. The study of patterns of variation of photoinduced processes with the protein environment of QDs is of particular interest for this QD type. The first barrier encountered by a nanoplatform in biological QD applications is opsonization (interaction with proteins of the circulatory system), which leads to the formation of a so-called protein corona on the QD surface [9]. This protein corona may affect the photophysical properties of NPs and their functionality; in particular, it may curb the potential for targeted delivery via surface modification of NPs. A protein corona of bovine fetal serum molecules will be used as a model of the protein environment of QDs in the bloodstream.

Albumin particles, which may be used for intracellular drug delivery, will be used as another protein environment model. Albumin nanocarriers have several advantages. This led to the approval of Abraxane, which is a conjugate of albumin and Paclitaxel designed for cancer therapy [10]. Encapsulation of QDs in albumin NPs will suppress the body's immune response to nanoplatforms. In addition, it will enable targeted delivery of QDs to cancer cells due to the interaction of albumin with gp60 and SPARC receptors of cancer cells [11] and enhance cellular internalization by changing the size of the system and their charge [12].

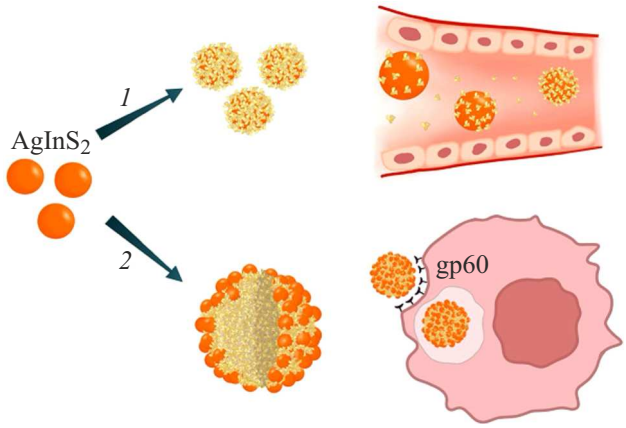

Figure 1. Schematic diagram of the systems based on QDs and protein molecules formed in the present study: *1* — conjugates with FBS that are meant to imitate the protein corona formed on the QD surface in the bloodstream; *2* — QDs encapsulated in ANPs that are capable of targeted delivery of QDs to cancer cells.

The study of photoinduced processes under the above conditions is a prerequisite for assessing the potential of QDs in bioimaging and photodynamic therapy.

In the present study, $AgInS_2$ and $AgInS_2/ZnS$ QDs were synthesized hydrothermally. Conjugates of QDs with serum and albumin NPs were produced by their coincubation for 24 h. It was found that a ZnS shell enhances the quantum yield of QD fluorescence and induces a hypsochromic shift of fluorescence spectra. The presence of proteins in the immediate environment reduces the quantum yield of QD fluorescence and also leads to a shift of QD fluorescence spectra to the short-wavelength region. $AgInS_2$ QDs are prone to rapid bleaching of fluorescent properties when exposed to external radiation; semiconductor (ZnS), protein (fetal bovine serum (FBS) proteins), and albumin shells slow down the rate of this process, making these systems better suited for biological applications.

Materials and methods

Aqueous $AgInS_2$ (core) and $AgInS_2/ZnS$ (core/shell) QDs were synthesized using the hydrothermal method [13]. The synthesis of $AgInS_2$ QDs was performed in a three-necked glass flask with 5 ml of H_2O. The following reagents were introduced into it successively: 0.052 ml of $AgNO_3$ (0.1 M), 0.104 ml of TGA (1 M), 0.0334 ml of NH_4OH (5 M), 0.0364 ml of $InCl_3$ (1 M), 0.08 ml of NH_4OH (5 M), and 0.052 ml of $Na_2S{\cdot}9H_2O$ (1 M). The synthesis lasted for 30 min. After that, 0.078 ml of TGA (1 M), 0.05 ml of NH_4OH (5 M), and $Zn(CH_3COO)_2$ (1.0 M) were added to grow the ZnS shell. The temperature of the medium in the flask was set to 90°C, remained constant throughout the process of synthesis, and was adjusted using a heating element and a temperature sensor in a water bath. Following synthesis, the QD solutions were washed by adding isopropyl alcohol in a 1:2 ratio and centrifuged for 3 min at 12 000 rpm. The samples were then re-dissolved in water and stored in the dark at a temperature of 4°C.

An aqueous solution of QDs with 10% and 30% FBS and a concentration of $5 \cdot 10^{-6}$ M was prepared in order to form conjugates of QDs with FBS proteins. The resulting mixture was left for coincubation for 15 h in the dark at room temperature. Albumin molecules, which are predominant in FBS, are negatively charged and bind electrostatically to positively charged QDs. The obtained conjugates were stored in the dark at a temperature of 4°C.

A similar technique was used to produce QD/albumin NP (ANP) systems. ANPs were synthesized by desolvation and subsequent cross-linking with glutaraldehyde [14]. The particles synthesized this way have a negative surface charge and a size of ~ 120 nm. A weighed portion (1 mg) of particles was added to the aqueous QD solution with a concentration of $5 \cdot 10^{-6}$ M. Coincubation was carried out in the dark at room temperature under constant stirring. The particles were then centrifuged for 15 min at 12 000 rpm, and free QDs remained in the non-settling liquid. The sedimented systems were re-dissolved in deionized water and stored in the dark at a temperature of 4°C. The QD encapsulation efficiency was estimated using the following formula:

$$E(\%) = (I_{initial} - I_{supernatant})/I_{inintial} \cdot 100\%,$$

where $I_{initial}$ and $I_{supernatant}$ are the fluorescence intensities of the QD solution at zero encapsulation time and of the supernatant during sedimentation of the systems at the end of encapsulation. The formed systems are shown schematically in Fig. 1.

The sizes of systems formed in the present study were assessed by dynamic light scattering using a Zetasizer Ultra device (Malvern Panalytical, United Kingdom). Stationary absorption and fluorescence spectra were recorded with a Multiskan Sky spectrophotometer (ThermoFisher Scientific, United States) and a Cary Eclipse spectrofluorimeter (Agilent, United States). The fluorescence quantum yield was estimated relative to rhodamine 6G.

To examine the effect of photoinduced processes on the surface of QDs on their fluorescent properties, the samples were exposed to UV radiation with a wavelength of 365 nm. The power incident on a sample was 0.3 mW; the cell with the sample was illuminated uniformly (the cross-sectional area of the cell was 1 cm^2). The sample was stirred periodically to ensure uniformity of QD exposure to external radiation. The total incident radiation dose was $\sim 0.75\ J{\circ}m^{-2}$. Fluorescence spectra of QDs and systems based on them were recorded periodically in the process of irradiation.

Results

The influence of photoinduced processes on the surface of QDs on their fluorescent properties was assessed in

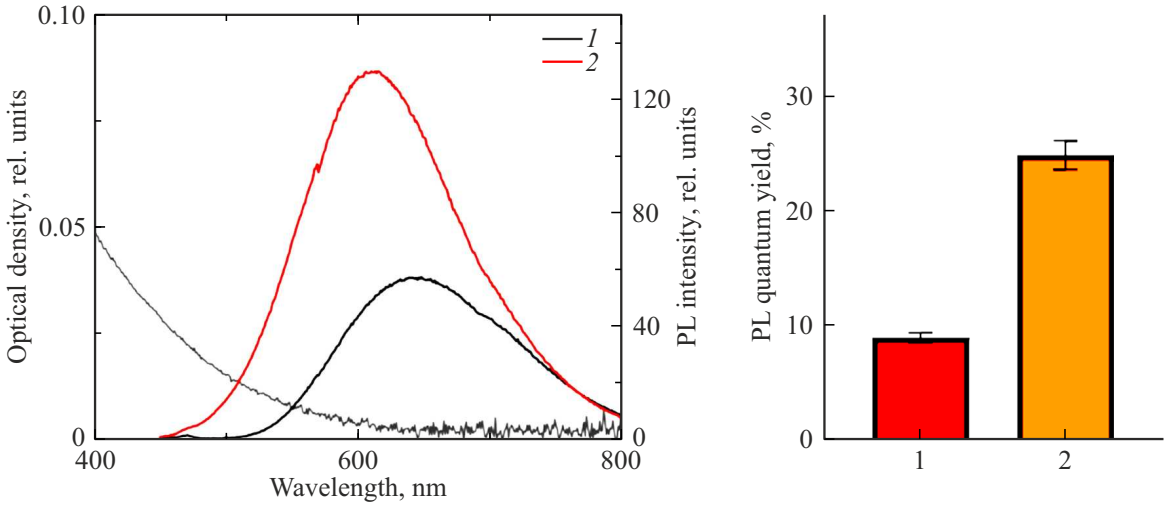

Figure 2. (*a*) Absorption and fluorescence spectra of $AgInS_2$ and $AgInS_2/ZnS$ QDs. The fluorescence excitation wavelength is 405 nm. (*b*) Quantum yield of $AgInS_2$ and $AgInS_2/ZnS$ QDs calculated relative to rhodamine 6G. *1* — $AgInS_2$ QDs, *2* — $AgInS_2/ZnS$ QDs.

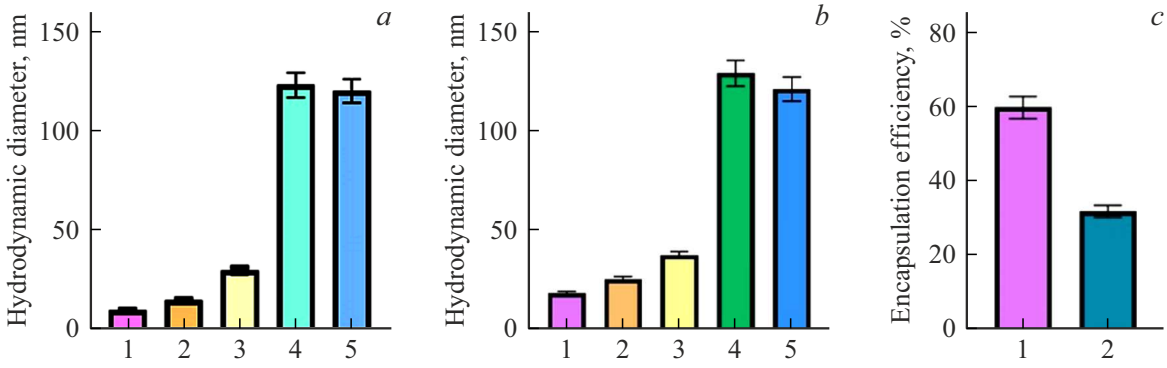

Figure 3. Hydrodynamic diameter of systems based on $AgInS_2$ (*a*) and $AgInS_2/ZnS$ (*b*) QDs: *1* — QD, *2* — QD/10FBS, *3* — QD/30FBS, *4* — QD/ANP, and *5* — ANP; efficiency of QD encapsulation in ANP: *1* — $AgInS_2$, *2* — $AgInS_2/ZnS$ (*c*).

three different model scenarios: an aqueous solution of QDs after synthesis ($AgInS_2$ and $AgInS_2/ZnS$), conjugates of QDs with FBS ($AgInS_2$/FBS and $AgInS_2/ZnS$/FBS), and systems with ANPs ($AgInS_2$/ANP and $AgInS_2/ZnS$/ANP). Each sample was characterized and exposed to external radiation. Fluorescence spectra of QDs were recorded in the process of irradiation.

The surface of QDs is characterized by the presence of a large number of defect states produced as a result of synthesis, which may act as carrier traps and reduce the quantum yield of QD fluorescence. It is possible to reduce the efficiency of these nonradiative relaxation channels of electron excitation by passivating the QD surface with ZnS (a wide-gap semiconductor). According to literature data, this should lead to an increase in quantum yield of QD fluorescence [15]. The absorption and fluorescence spectra of $AgInS_2$ and $AgInS_2/ZnS$ QDs are shown in Fig. 2.

It can be seen from Fig. 2 that the growth of a shell led to a hypsochromic shift of the fluorescence spectrum of $AgInS_2$ QDs to the short-wavelength region (from 645 to 630 nm) accompanied by a more than 2.5-fold increase in quantum yield of fluorescence (from 9 to 24%), which agrees closely with literature data. However, this results in a shift of the absorption region of QDs away from the transparency window of the human body (650–950 nm), hindering their functionality *in vivo*. When QDs enter the bloodstream, their surface is coated with a layer of proteins (the so-called protein corona), which may lead to a significant alteration of their luminescent and photophysical properties. In addition, albumin particles are planned to be used in future work for intracellular delivery of QDs to increase the efficiency of photodynamic therapy through the generation of a superoxide.

The method for forming the protein environment was detailed above (see Materials and Methods). Figure 3 presents the dimensions of the formed systems determined by dynamic light scattering and the efficiency of QD encapsulation in albumin particles.

It can be seen that when QDs are incubated in a solution containing 10 and 30% FBS, the system size increases

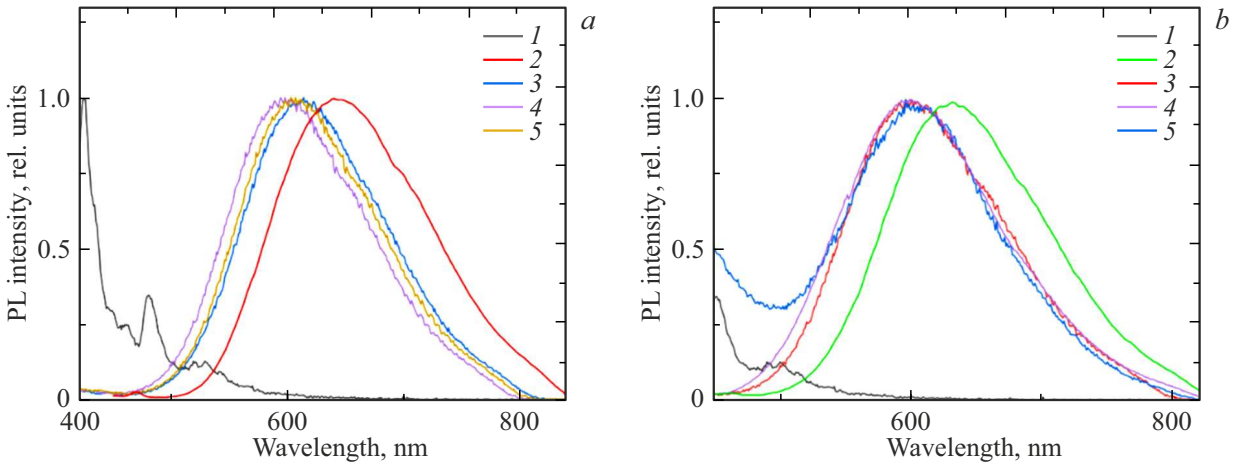

Figure 4. Fluorescence spectra of systems based on $AgInS_2$ (*a*) and $AgInS_2$/ZnS (*b*) QDs: *1* — ANP, *2* — QD, *3* — QD/10FBS, *4* — QD/30FBS, and *5* — QD/ANP. The fluorescence excitation wavelength is 405 nm.

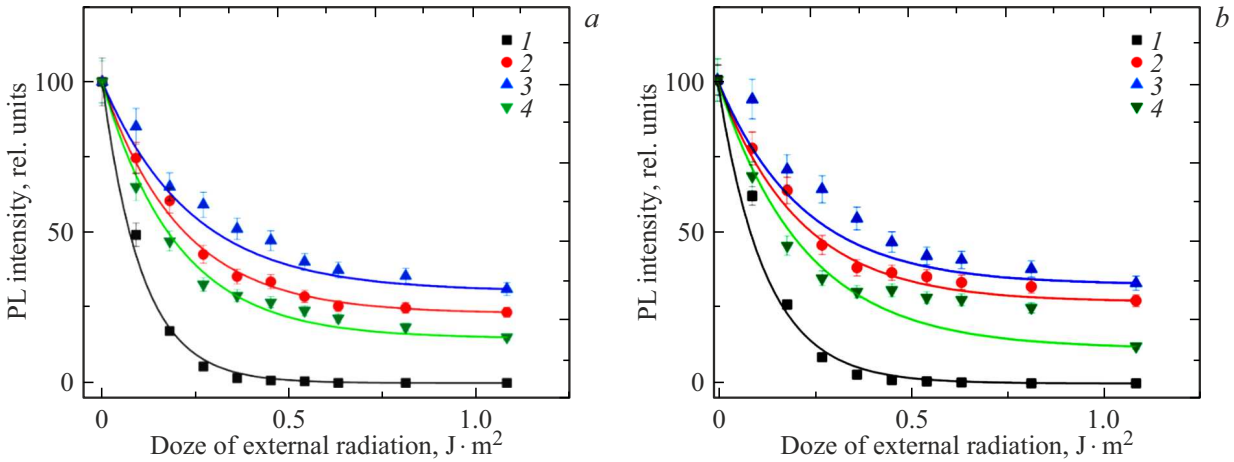

Figure 5. Variation of QD fluorescence during long-term irradiation for systems based on $AgInS_2$ (*a*) and $AgInS_2$/ZnS (*b*) QDs: *1*— QD, *2* — QD/10FBS, *3* — QD/30FBS, and *4* — QD/ANP. The data are normalized to the fluorescence intensity at the initial moment of irradiation.

significantly, and this increase is correlated with the FBS content. Specifically, the $AgInS_2$ QD system grew in size by a factor of 3 (from 10 to 30 nm) after incubation in the 30% FBS solution. In this case, when QDs are administered intravenously into the body, proteins will constitute more than 70% of the QD/protein corona system volume and will govern the surface properties of the resulting system and the nano-bio-interaction. As for QD/ANP systems, their size is determined by the size of the initial ANPs (120 nm), and QD encapsulation leads to a slight increase in hydrodynamic diameter (up to 125 and 128 nm) with an $AgInS_2$ and $AgInS_2$/ZnS QD encapsulation efficiency of 60% and 32%, respectively. It may be assumed that QDs were embedded in the surface layer of albumin particles, and targeted delivery of QDs to cancer cells due to activation of transport through gp60 receptors and binding to the secreted SPARC protein is still possible in this case [11].

Presumably, the protein environment should influence the quantum yield of the formed systems and the photophysical properties of QDs. Figure 4 shows the normalized fluorescence spectra of QD-based systems.

It can be seen from Fig. 4 that the protein environment induces a significant shift of fluorescence spectra to the short-wavelength region. According to literature data, the observed hypsochromic shift of fluorescence spectra is associated with a change in the surface charge of QDs, which becomes more negative [16]. Notably, the protein shell of QDs and albumin particles induce the same change in spectra, which confirms this hypothesis. All the formed systems were subjected to long-term UV irradiation, but no significant spectral shifts of the QD fluorescence band were observed in the process. Figure 5 presents the variation of intensity of QD fluorescence during irradiation.

It can be seen from Fig. 5 that the irradiation of QDs leads to a reduction in their fluorescence intensity. With no noted

changes in the absorption spectra of QDs, this is indicative of a reduction in the quantum yield of QD fluorescence. The rapid changes observed under irradiation for both QD types provide evidence of the formation of new relaxation channels that compete with fluorescence.

A slight enhancement of QD fluorescence intensity ($\leq 5\%$) was noted at a total incident radiation dose below $15\,mJ{\cdot}m^2$. According to literature data, the fluorescence of $AgInS_2$ QDs is defect-based, which leads to long characteristic fluorescence decay times [17]. A rapid fluorescence intensity reduction may then be indicative of photochemical passivation of fluorescent centers of the QDs. The ZnS shell slows down slightly the photobleaching process at low irradiation doses ($0.25\,J{\cdot}m^2$), but even then the QDs lose their fluorescent properties rather quickly (Fig. 5, *b*). The protein environment induces a significant slowdown of these processes, potentially allowing one to preserve the functionality of QDs for a long period of time. Specifically, when the incident radiation dose exceeds $0.4\,J{\cdot}m^2$, QDs demonstrate complete photoinduced quenching of luminescence, while the fluorescence intensity with the protein environment remains at a level of 25% of the initial one even at higher doses.

It follows from Fig. 5 that conjugation with serum proteins was more efficient in protecting against photoinduced changes in the surface properties of QDs than their encapsulation in albumin particles.

Conclusions

The obtained data demonstrate that the protein environment formed when QDs enter the circulatory system and interact with cells will exert a significant influence on the photophysical properties of QDs. Specifically, conjugation with blood proteins and encapsulation in albumin particles induces a hypsochromic shift of fluorescence of QDs and a reduction in the fluorescence quantum yield, hindering their use *in vivo*. However, the protein environment provides an opportunity to reduce significantly the efficiency of photoinduced bleaching of the fluorescent properties of QDs and preserve their functionality. Efficient application of QDs in biology requires optimization of QD synthesis aimed at shifting the absorption spectral region to the near IR range.

Funding

This study was supported by the Russian Science Foundation, project № 24-24-20102.

Conflict of interest

The authors declare that they have no conflict of interest.

References

[1] D.S. Kumar, B.J. Kumar, H.M. Mahesh. Synthesis of Inorganic Nanomaterials, **59**–**88** (2018). DOI: 10.1016/B978-0-08-101975-7.00003-8
[2] F.P. García de Arquer, D.V. Talapin, V.I. Klimov, Y. Arakawa, M. Bayer, E.H. Sargent. Science, **373** (6555), eaaz8541 (2021). DOI: 10.1126/science.aaz8541
[3] V.K. Sharma, T.J. McDonald, M. Sohn, G.A. Anquandah, M. Pettine, R. Zboril. Chemosphere, 188, 403 (2017). DOI: 10.1016/j.chemosphere.2017.08.130
[4] A. Lin, X.H. Zhang, M.M. Chen, Q. Cao. J. Env. Sc., **19** (5), 596 (2007). DOI: 10.1016/S1001-0742(07)60099-0
[5] J.Y. Chang, G.Q. Wang, C.Y. Cheng, W.X. Lin, J.C. Hsu. J. Mat. Chem., **22** (21), 10609 (2012). DOI: 10.1039/C2JM30679D
[6] K.N. Baranov, E.P. Kolesova, M.A. Baranov, A.O. Orlova. Opt. Spectrosc., **130** (5), 336 (2022). DOI: 10.1134/S0030400X22060017
[7] S.F. Lee, M.A. Osborne. ChemPhysChem, **10** (13), 2174 (2009). DOI: 10.1002/cphc.200900200
[8] E.P. Kolesova, F.M. Safin, V.G. Maslov, Y.K. Gun'ko, A.O. Orlova. Opt. Spectrosc., **127**, 548 (2019). DOI: 10.1134/S0030400X19090157
[9] W. Kim, N.K. Ly, Y. He, Y. Li, Z. Yuan, Y. Yeo. Adv. Drug Delivery Rev., **192**, 114635 (2023). DOI: 10.1016/j.addr.2022.114635
[10] A. Spada, J. Emami, J.A. Tuszynski, A. Lavasanifar. Mol. Pharmaceutics, **18** (5), 1862 (2021). DOI: 10.1021/acs.molpharmaceut.1c00046
[11] Q. Ji, H. Zhu, Y. Qin, R. Zhang, L. Wang, E. Zhang, R. Meng. Frontiers in Pharmacology, **15**, 1329636 (2024). DOI: 10.3389/fphar.2024.1329636/full
[12] A.M. Bannunah, D. Vllasaliu, J. Lord, S. Stolnik. Mol. Pharmaceutics, **11** (12), 4363 (2014). DOI: 10.1021/mp500439c
[13] A. Raevskaya, V. Lesnyak, D. Haubold, V. Dzhagan, O. Stroyuk, N. Gaponik, A. Eychm?ller. J. Phys. Chem. C, **121** (16), 9032 (2017). DOI: 10.1021/acs.jpcc.7b00849
[14] E.P. Kolesova, V.S. Egorova, A.O. Syrocheva, A.S. Frolova, D. Kostyushev, A. Kostyusheva, A. Parodi. Int. J. Mol. Sci., **24** (12), 10245 (2023). DOI: 10.3390/ijms241210245
[15] I.A. Mir, M.A. Bhat, Z. Muhammad, S.U. Rehman, M. Hafeez, Q. Khan, L. Zhu. J. Alloys and Compounds, **811**, 151688 (2019). DOI: 10.1016/j.jallcom.2019.151688
[16] L. Lai, C. Lin, Z.Q. Xu, X.L. Han, F.F. Tian, P. Mei, Y. Liu. Spectrochim. Acta Part A: Mol. Biomol. Spectrosc., **97**, 366 (2012). DOI: 10.1016/j.saa.2012.06.025
[17] C. Rivaux, T. Akdas, R. Yadav, O. El-Dahshan, D. Moodelly, W.L. Ling, P. Reiss. J. Phys. Chem. C, **126** (48), 20524 (2022). DOI: 10.1021/acs.jpcc.2c06849

Translated by D.Safin